Ferrata Storti Foundation

Arrayed molecular barcoding identifies TNFSF13 as a positive regulator of acute myeloid leukemia-initiating cells

Marion Chapellier,[1] Pablo Peña-Martínez,[1] Ramprasad Ramakrishnan,[1] Mia Eriksson,[1] Mehrnaz Safaee Talkhoncheh,[2] Christina Orsmark-Pietras,[1] Henrik Lilljebjörn[1], Carl Högberg,[1] Anna Hagström-Andersson,[1] Thoas Fioretos,[1] Jonas Larsson,[2] and Marcus Järås[1]

[1]Department of Clinical Genetics and [2]Molecular Medicine and Gene Therapy, Lund Stem Cell Center, Lund University, Lund, Sweden

Haematologica 2019
Volume 104(10):2006-2016

ABSTRACT

Dysregulation of cytokines in the bone marrow (BM) microenvironment promotes acute myeloid leukemia (AML) cell growth. Due to the complexity and low throughput of *in vivo* stem-cell based assays, studying the role of cytokines in the BM niche in a screening setting is challenging. Here, we developed an *ex vivo* cytokine screen using 11 arrayed molecular barcodes, allowing for a competitive *in vivo* readout of leukemia-initiating capacity. With this approach, we assessed the effect of 114 murine cytokines on *MLL-AF9* AML mouse cells and identified the tumor necrosis factor ligand superfamily member 13 (TNFSF13) as a positive regulator of leukemia-initiating cells. By using *Tnfsf13*$^{-/-}$ recipient mice, we confirmed that TNFSF13 supports leukemia initiation also under physiological conditions. TNFSF13 was secreted by normal myeloid cells but not by leukemia mouse cells, suggesting that mature myeloid BM cells support leukemia cells by secreting TNFSF13. TNFSF13 supported leukemia cell proliferation in an NF-κB-dependent manner by binding TNFRSF17 and suppressed apoptosis. Moreover, TNFSF13 supported the growth and survival of several human myeloid leukemia cell lines, demonstrating that our findings translate to human disease. Taken together, using arrayed molecular barcoding, we identified a previously unrecognized role of TNFSF13 as a positive regulator of AML-initiating cells. The arrayed barcoded screening methodology is not limited to cytokines and leukemia, but can be extended to other types of *ex vivo* screens, where a multiplexed *in vivo* read-out of stem cell functionality is needed.

Correspondence:

MARCUS JÄRÅS
marcus.jaras@med.lu.se

Received: February 27, 2018.

Accepted: February 21, 2019.

Pre-published: February 28, 2019.

doi:10.3324/haematol.2018.192062

Check the online version for the most updated information on this article, online supplements, and information on authorship & disclosures: www.haematologica.org/content/104/10/2006

Introduction

Acute myeloid leukemia (AML) is characterized by an accumulation of immature myeloid blasts in the bone marrow (BM).[1] By providing cell-cell interactions and secreted factors, the BM niche supports AML and normal hematopoietic stem and progenitor cells (HSPC).[1,2] A dysregulation of cytokines in the BM microenvironment upon AML development contributes to the selective advantage of leukemia stem cells,[1] a self-renewing population of leukemia cells that constitutes a chemoresistant reservoir responsible for disease relapse.[3]

To identify factors that regulate AML cells, we recently developed an *in vitro* cytokine screen using fluorescently labeled c-Kit^{+} leukemia cells mixed with corresponding normal BM cells, allowing us to successfully identify both negative and positive regulators of AML cells.[4] However, to assess effects on leukemia stem cells, there is a strong demand to improve such screens to evaluate the impact of cytokines on the leukemia-initiating capacity of cells more directly using an *in vivo* readout. A major challenge for combining *ex vivo* screens with *in vivo* read-out of stem cell function is the large number of experimental animals needed to provide meaningful data. Hence, new methods that allow for a multiplexed *in vivo* read-out

of leukemia-initiating activity are needed. Molecular barcoding strategies, combined with next-generation sequencing (NGS), enable an *in vivo* readout of stem cell function in a competitive setting.[5-7] By using this strategy, the *in vivo* cell fate of multiple hematopoietic stem cells (HSC) or leukemia clones can be monitored on a clonal level.[5,8] However, because these approaches use pooled barcoded libraries, the *in vivo* cell fate of the genetically marked stem cell clones within mice cannot be traced to separate experimental conditions, such as cytokine stimulations.

In this study, we created a library of 11 arrayed molecular barcodes that were used to mark leukemia cells exposed to 114 separate cytokine conditions. The 11 barcoded leukemia cell populations were then pooled and injected into mice allowing for an *in vivo* competition read-out of leukemia-initiating activity. By using this methodology, we identified the tumor necrosis factor ligand superfamily member 13 (TNFSF13; also named, A proliferation-inducing ligand, APRIL) as a novel positive regulator of leukemia-initiating cells. TNFSF13 promoted AML cell growth by suppressing apoptosis and activating nuclear factor kappa B (NF-κB).

Methods

Murine leukemia model

MLL-AF9 (KMT2A-MLLT3) leukemias were generated on a *dsRed*$^+$ C57BL/6 transgenic background (6051; Jackson Laboratory, Bar Harbor, ME, USA), as previously described.[9,10] Experiments involving murine leukemia cells were performed using tertiary or quaternary transplanted leukemia cells serially propagated in sublethally irradiated (600 cGy) recipient mice. All animal experiments were conducted according to an Animal Care and Use Committee protocol approved by the Lund/Malmö Ethical Committee. Except for the propagation of leukemia cells, all experiments involving murine leukemia cells were performed using c-Kit$^+$ bone marrow cells. For details on the c-Kit$^+$ cells isolation and cell culture conditions, see the *Online Supplementary Methods.*

Generation of 11 lentiviral vectors containing molecular barcodes

To generate lentiviral vectors containing non-expressed molecular barcodes, we used a lentiviral pLKO.1 vector (Addgene #32684) that co-expressed a short hairpin RNA (shRNA) and a green fluorescent protein (GFP) marker gene.[11] The shRNA sequence, along with its promotor, was replaced by genetic barcodes (42 to 46 nucleotides) flanked by 23mer primer sequences using the *Nde1* and *EcoR1* restriction sites (*Online Supplementary Table S1*). Viral vectors with VSV-g pseudotyping were produced using standard protocols.

Ex vivo cytokine screening using barcoded leukemia cells

Freshly isolated c-Kit$^+$ dsRed$^+$ leukemia cells were transduced with the barcoded lentiviral vectors and exposed to the cytokine library of 114 cytokines (*Online Supplementary Table S2*) in 96-well plates. After 72 hours, cells from different wells were pooled, with each pool containing leukemia cells from up to 11 barcoded populations representing specific culture conditions, and injected into sublethally irradiated (600 cGy) recipient C57BL/6 mice *via* tail vein injection. After 7-12 days, mice were sacrificed, BM cells were harvested, and DNA was extracted (Qiagen Blood and Tissue DNA Extraction Kit). For details on the screen see the *Online Supplementary Methods*.

Sequencing of barcodes and bioinformatics analysis

Following BM cell extraction and DNA purification (DNAeasy Blood and Tissue Kit, Qiagen), the regions containing the barcodes were amplified using two-step polymerase chain reaction (PCR). Step one utilized pLKO.1-specific primers containing Nextera overhangs (*Online Supplementary Table S3*). The number of reads per barcode of each sample was extracted and normalized to the total read count within each sample. The mean of the three biological replicates was then calculated after normalization to the input (Day 0). For further details on the sequencing and bioinformatics, see the Online *Supplementary Methods*.

Tnfsf13$^{-/-}$ mouse model

The C57BL/6 *Tnfsf13*$^{-/-}$ mouse (#022971; B6.*Cg-Tnfsf13tm1Pod/J*)[12,13] was obtained from The Jackson Laboratory (Bar Harbor, Maine, USA) and further backcrossed (>5 generations) onto C57BL/6 wild-type mice. Genotyping was performed by PCR using protocols provided by the Jackson Laboratory.

Retroviral *MLL-AF9* expression in c-Kit$^+$ bone marrow cells and transplantations into sublethally irradiated mice

Murine stem cell virus gammaretroviral vectors co-expressing *MLL-AF9* and *GFP* (MIG-MLL-AF9)[14] were produced with an ecotropic envelope using standard protocols in 293T cells. c-Kit$^+$ BM cells were pre-stimulated for two days and spinoculated. Following overnight incubation at 37°C, transduced cells were injected into sublethally irradiated (600 cGy) recipient mice *via* tail vein injection. Each recipient mouse received cells corresponding to 250,000 initially seeded cells. Blood samples were taken after 40 days, and mice were sacrificed when they showed signs of disease. To assess leukemia development in sublethally irradiated (600 cGy) secondary recipient mice, 1,000 or 10,000 spleen leukemia cells from primary recipients were injected *via* the tail vein. For details on the transduction of c-Kit$^+$ BM cells, see the *Online Supplementary Methods.*

Flow cytometric analysis and cell sorting

The flow cytometric analyses were performed using a FACS Canto II (BD Biosciences, San Jose, CA, USA) or a FACS LSRFortessa (BD Biosciences), and cell sorting was performed using a FACS Aria II (BD Biosciences). For detailed information on antibodies used and staining for LSK and HSPC analysis, cell cycle, apoptosis and phosphoflow, see the *Online Supplementary Methods*.

Statistical analysis

Prism 6 (Graphpad) was used for the statistical analyses, including Student *t*-test and Kaplan-Meier survival analysis. Statistical significance is shown with asterisks: $^*P<0.05$; $^{**}P<0.01$; $^{***}P<0.001$; $^{****}P<0.0001$. Data are presented as mean±Standard Deviations (SD).

Results

Development of an *ex vivo* cytokine screen with a competitive *in vivo* read-out of leukemia-initiating activity using molecularly barcoded leukemia cells

To identify cytokines that regulate AML stem cells using a competitive *in vivo* read-out of leukemia-initiating activity, we generated lentiviral vectors harboring genetic barcodes in an arrayed setting. This approach allows for

labeling of leukemia cell populations with distinct molecular barcodes followed by exposure to separate experimental conditions. Each labeled cell population was stimulated with one cytokine *ex vivo* and after culture, leukemia cells from multiple cytokine conditions were pooled prior to *in vivo* competition. To trace the effects of the cytokines to the leukemia-initiating capacity of barcoded cells, the representation of individual barcodes *in vivo* was assessed using NGS (Figure 1A).

To allow for *in vivo* competition of up to 11 barcoded cell populations, we generated 11 lentiviral vectors with unique molecular barcodes and GFP as a marker gene (*Online Supplementary Table S1*). The barcodes were used to mark c-Kit$^+$ murine *MLL-AF9* AML cells generated on a dsRed transgenic background (Figure 1A and *Online Supplementary Figure S1A*). We have previously used these cells in screens because they have a well-defined leukemia-initiating cell population and initiate AML with a short latency, enabling rapid follow-up experiments in syngeneic hosts.[4,9,10,14,15]

To validate the robustness of the new methodology, 11 barcoded c-Kit$^+$ leukemia cell populations were exposed separately for three days to stem cell factor (SCF), which binds c-Kit and activates signaling that promotes leukemia-initiating cells.[16] Leukemia cells from the 11 barcoded cell populations were then pooled and injected into sublethally irradiated mice for *in vivo* competition of leukemia-initiating activity. Seven days post transplantation, mice were sacrificed, their BM was harvested, and DNA was extracted. We found that the 11 barcoded variants showed a similar distribution with less than 2-fold variability in the input pool relative to the *in vivo* pool (range: 0.51- to 1.65-fold), demonstrating that the arrayed barcoding methodology was robust in assessing the leukemia-initiating activity of the AML cells following *ex vivo* culture (Figure 1B).

Identification of TNFSF13 as a positive regulator of acute myeloid leukemia-initiating cells

To assess the impact of a library of 114 murine cytokines on c-Kit$^+$ MLL-AF9 leukemia cells, we performed two arrayed *ex vivo* cytokine screens, in which each cytokine was assessed in triplicate wells (*Online Supplementary Table S2*). After three days of *ex vivo* cytokine stimulation, up to 11 cytokine conditions of barcoded leukemia cells were pooled and injected into recipient mice (Figure 1A). As an internal positive control, for each pool, we stimulated one of the barcoded cell populations with SCF. The mice were sacrificed on day 7 (screen I) or day 12 (screen II) post transplantation, and engraftment of transduced leukemia cells was confirmed by assessing the frequency of GFP positive cells within dsRed$^+$ cells (*Online Supplementary Figure S1B and C*). As predicted, barcoded leukemia cells stimulated with SCF

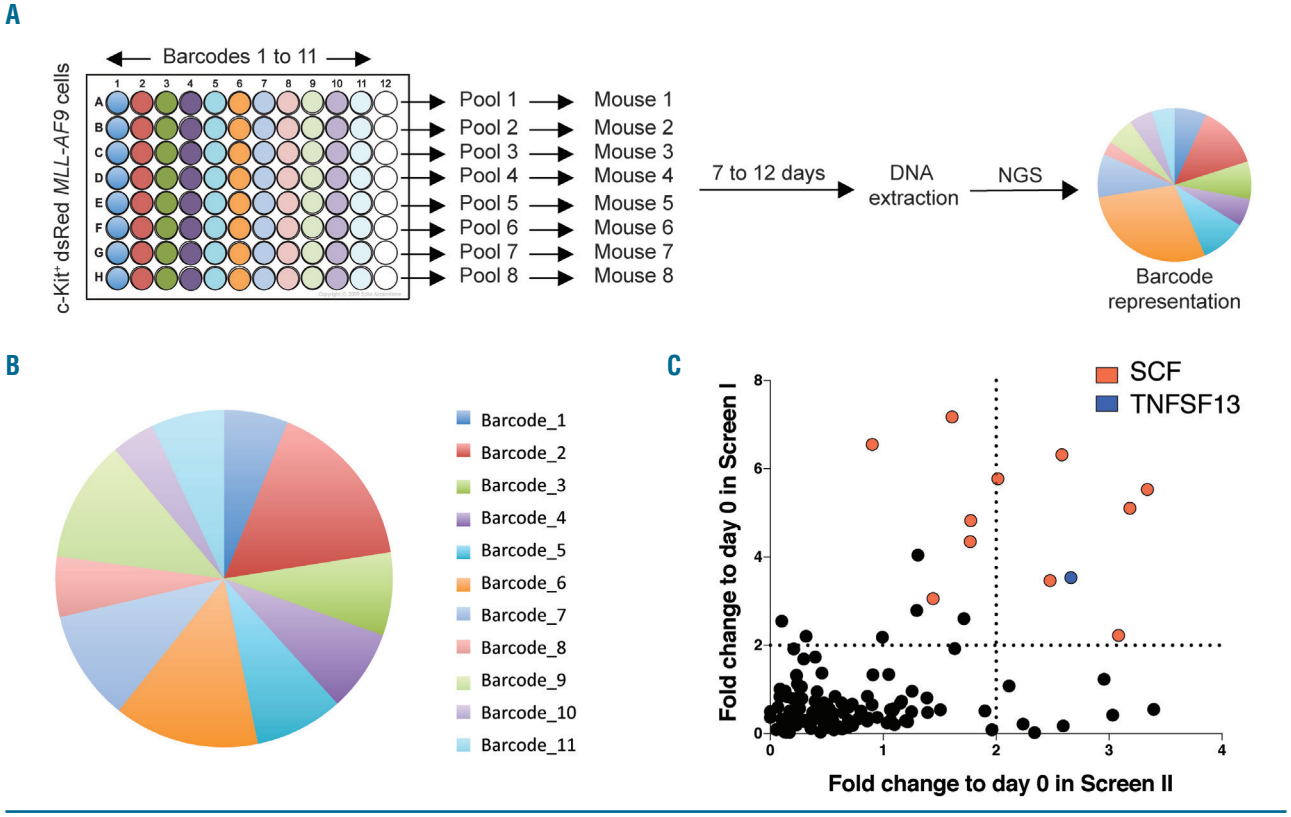

Figure 1. A barcoded cytokine screen identifies TNFSF13 as a positive regulator of acute myeloid leukemia (AML)-initiating cells. (A) Schematic flowchart depicting the arrayed barcoded *ex vivo* cytokine screen with AML cells. In total, 12 pools in triplicate were used to screen the entire cytokine library. After seven (screen I) or 12 (screen II) days, mice were sacrificed. Data were normalized to the input representation for each barcode. (B) Pie chart displaying the contribution of each barcoded cell population *in vivo* following *ex vivo* cultures with stem cell factor (SCF) only for all barcoded cell populations. (C) Scatter plot showing fold-change *in vivo versus* input of barcoded cell populations for the two screens. Dotted lines represent a fold-change threshold of 2 to identify cytokines that promote leukemia-initiating cells. Red dots: barcoded cell populations stimulated *ex vivo* with SCF as the positive control within each pool; blue dots: cells stimulated with TNFSF13. NGS: next-generation sequencing.

showed a relative increase within all pools *in vivo*, thus validating the new method (Figure 1C). Although a number of cytokines, such as interleukin-3 (IL3) and granulocyte-macrophage colony-stimulating factor (GM-CSF), that greatly expand (>20-fold over 3 days) AML cells in culture were included in the screen,[4] none of them expanded the leukemia-initiating cell population as assessed with *in vivo* read-out (*Online Supplementary Table S3*). This finding highlights the need for *in vivo* readout to assess the impact of cytokines on the leukemia-initiating capacity of the cells. Setting a threshold for 2-fold enrichment, TNFSF13 was the only cytokine, other than SCF, that scored in both screens (on average a 3.1-fold relative increase). In addition, the screens identified Interleukin 9 (IL9) as a candidate positive regulator (1.8 relative increase) of leukemia-initiating cells (*Online Supplementary Table S2*). Moreover, several negative regulators of leukemia-initiating cells were identified that were not further investigated in the present study (*Online Supplementary Table S2*).

Ex vivo stimulation with TNFSF13 or IL9 promotes leukemia-initiating cells

To validate the findings from the screen and first explore TNFSF13 as a regulator of primitive AML cells, we cultured c-Kit$^+$ *MLL-AF9* leukemia cells with increasing doses of TNFSF13. TNFSF13 supported the growth and survival of c-Kit$^+$ leukemic cells in culture (Figure 2A and *Online Supplementary Figure S2A*), but did not affect normal HSPC, as assessed by analyzing the effect of TNFSF13 on Lin$^-$Sca-1$^+$ c-Kit$^+$ (LSK) BM cells from healthy mice (Figure 2B). Moreover, *ex vivo* stimulation of c-Kit$^+$ leukemia cells with TNFSF13, followed by transplantation into sublethally irradiated mice, resulted in significantly higher levels of circulating leukemia cells in peripheral blood (mean 25.6% *vs.* 1.3% for non-stimulated cells; $P<0.0001$) (Figure 2C and D). Notably, the numbers of circulating leukemia cells were even higher than for mice that had received leukemia cells that were stimulated with SCF as a positive control (25.6% *vs.* 7.8%; $P<0.01$) (Figure 2D). Consistent with this finding, the TNFSF13-treated group exhibited reduced survival (median survival 29 *vs.* 38 days for the non-stimulated group; $P<0.0001$) (Figure 2E) and survival was even slightly shorter than for the SCF-treated group (Figure 2E). At the time of sacrifice, all except for one control mouse had a high leukemic burden, as confirmed by enlarged spleens and a high percentage of leukemia cells (>95% dsRed$^+$ cells) in their BM (*Online Supplementary Figure S2B and C*). Consistent with the findings in the

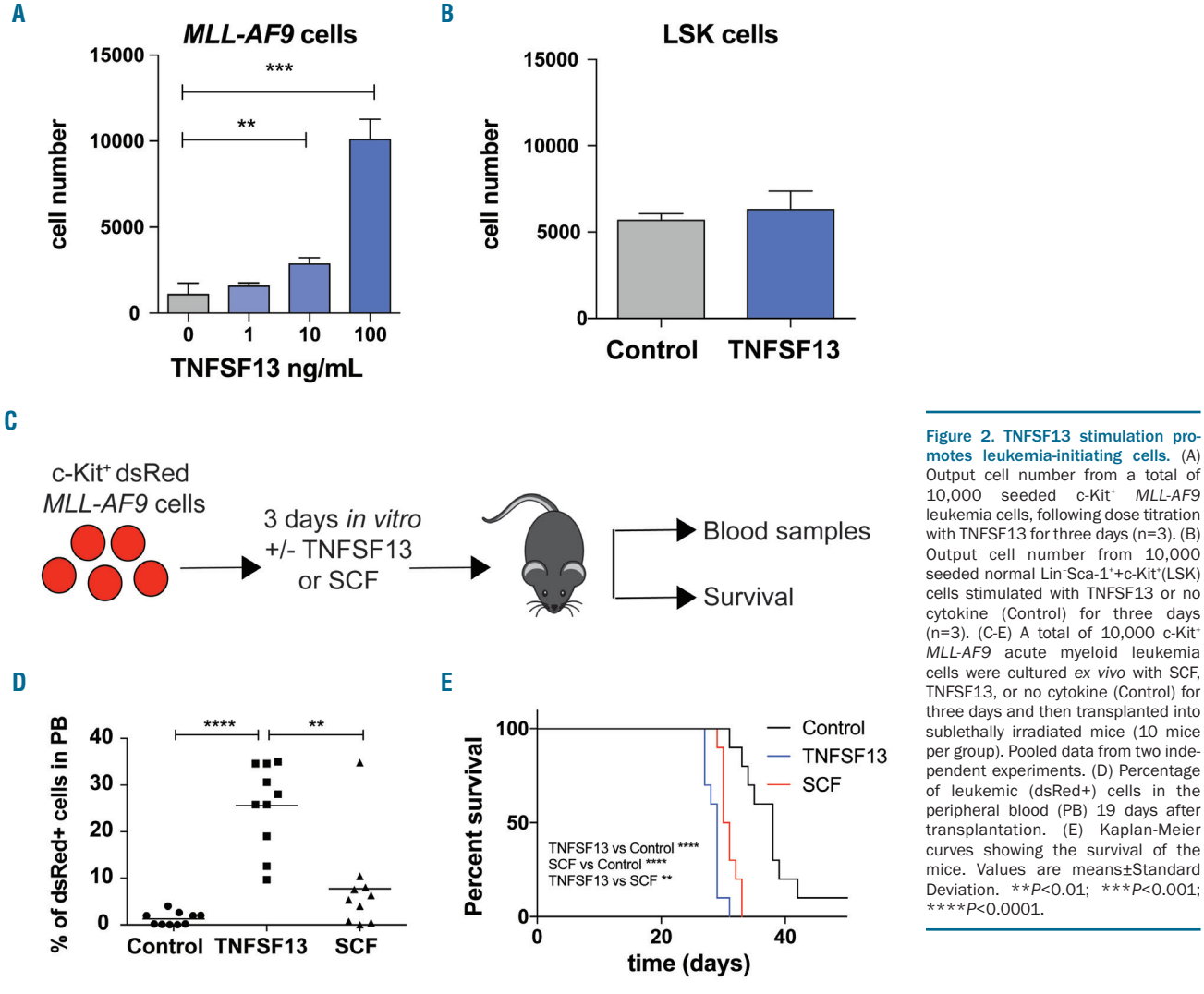

Figure 2. TNFSF13 stimulation promotes leukemia-initiating cells. (A) Output cell number from a total of 10,000 seeded c-Kit$^+$ *MLL-AF9* leukemia cells, following dose titration with TNFSF13 for three days (n=3). (B) Output cell number from 10,000 seeded normal Lin$^-$Sca-1$^+$+c-Kit$^+$(LSK) cells stimulated with TNFSF13 or no cytokine (Control) for three days (n=3). (C-E) A total of 10,000 c-Kit$^+$ *MLL-AF9* acute myeloid leukemia cells were cultured *ex vivo* with SCF, TNFSF13, or no cytokine (Control) for three days and then transplanted into sublethally irradiated mice (10 mice per group). Pooled data from two independent experiments. (D) Percentage of leukemic (dsRed+) cells in the peripheral blood (PB) 19 days after transplantation. (E) Kaplan-Meier curves showing the survival of the mice. Values are means±Standard Deviation. $^{**}P<0.01$; $^{***}P<0.001$; $^{****}P<0.0001$.

screen, IL9 also supported the growth of leukemic cells *in vitro* (*Online Supplementary Figure S3A*) and *ex vivo* stimulation of c-Kit$^+$ leukemia cells with IL9 prior to transplantation into mice resulted in elevated levels of leukemia cells in the blood and reduced survival compared to controls (*Online Supplementary Figure S3B and C*). Taken together, these observations validate our barcoded screening strategy and demonstrate that primarily TNFSF13, but also IL9, support AML-initiating cells.

Myeloid cells secrete TNFSF13

To assess the *in vivo* relevance of TNFSF13 in the context of AML, we measured TNFSF13 levels in the peripheral blood (PB) and BM of healthy control and leukemic mice. TNFSF13 was present at physiologically relevant levels in the PB and BM of both leukemic and healthy mice but at significantly higher levels in the blood of healthy control mice (Figure 3A and B). To determine whether TNFSF13 is secreted by AML cells or provided by cells in the microenvironment, normal c-Kit$^+$ cells and AML BM cells were cultured for three days in suspension cultures under conditions favoring myeloid (Gr-1$^+$CD11b$^+$) cell growth (Figure 3C), and *TNFSF13* expression in cells and TNFSF13 levels in the supernatants were analyzed. We found that normal myeloid BM cells expressed high levels of TNFSF13 (>240 ng/mL in supernatant), whereas leukemic cells did not (<10 ng/mL in supernatant), suggesting that non-leukemic myeloid cells support AML cells by secreting TNFSF13 (Figure 3D and E).

Tnfsf13$^{-/-}$ mice have myelopoiesis defects

To investigate the physiological role of TNFSF13 in an *in vivo* context, we used *Tnfsf13*$^{-/-}$ mice, which previously have mainly been characterized regarding cytokine regu-

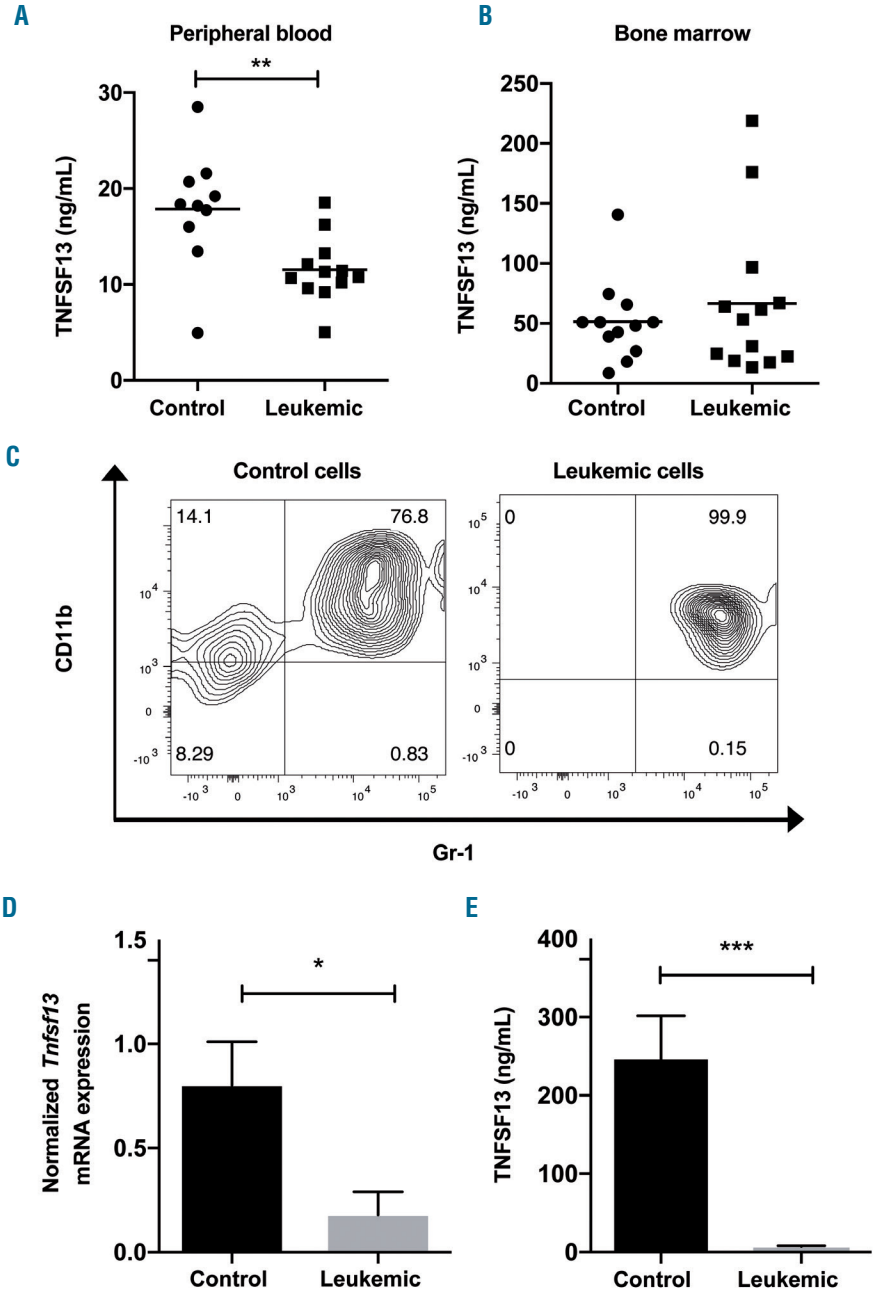

Figure 3. TNFSF13 is present in the bone marrow and peripheral blood and is secreted by myeloid cells. ELISA quantification of TNFSF13 in (A) blood plasma samples from healthy (10 mice) and leukemic mice (12 mice) and (B) bone marrow samples from healthy (12 mice) and leukemic mice (13 mice). (C-E) c-Kit$^+$ normal (control) and c-Kit$^+$ leukemic bone marrow cells were cultured for three days under conditions favoring myeloid cell growth. (C) Representative dot plots showing expression of CD11b and Gr-1 on control and leukemic bone marrow cells after three days of culture. (D) *Tnfsf13* mRNA expression in control and leukemic bone marrow cells determined by real-time polymerase chain reaction and normalized to a control sample after three days of culture (n=3 per group). (E) ELISA quantification of TNFSF13 in supernatants of normal or leukemic c-Kit$^+$ bone marrow cells cultured for three days (n=8 per group). Values are means±Standard Deviation. *P<0.05; **P<0.01; ***P<0.001.

lation and T-cell biology.[12,13] No change in white blood cell count, red blood cell count, or platelet levels was observed in *Tnfsf13*$^{-/-}$ mice (*Online Supplementary Table S4*). We then characterized their HSPC compartment and the lineage distribution in the BM and PB (*Online Supplementary Figure S4A and B*). Whereas long- and short-term HSC numbers were not affected, a significant decrease in granulocyte and macrophage progenitor (GMP) cells, accompanied by reduced numbers of monocytes, and a trend towards lower levels of granulocytes, was observed (Figure 4A-D, *Online Supplementary Table S4* and *Online Supplementary Figure S4A and B*). Moreover, a skewing towards more B cells and fewer T cells was detected in the BM, whereas in the PB, only T cells were significantly altered (*Online Supplementary Table S4*). These data indicate that TNFSF13 supports the formation of GMP cells and that it favors myeloid and T-cell development relative to B cells.

TNFSF13 is a ligand for two cell-surface receptors: TNF receptor superfamily member 13B (TNFRSF13B) and 17 (TNFRSF17).[17] Whereas TNFRSF17 was expressed on c-Kit^{+} leukemia cells, these cells were devoid of TNFRSF13B expression (Figure 4E and F). On normal HSPC, and in mature lineages of the BM and PB, TNFRSF17 was more broadly expressed than TNFRSF13B (Figure 4G and H and *Online Supplementary Figure S4C-G*). TNFRSF17 expression was detected in several mature blood cell lineages and multiple progenitor cell populations, with the lowest expression detected on long-term HSC (Figure 4G and H and *Online Supplementary Figure S4C and D*). These data suggest that TNFRSF17 is the primary receptor for TNFSF13 on murine AML cells and a putative receptor for TNFSF13 on normal murine myeloid progenitor cells and monocytes.

TNFSF13 promotes acute myeloid leukemia initiation by suppressing apoptosis and promoting active cell cycle progression

To assess whether TNFSF13 supports leukemia-initiation and progression *in vivo*, c-Kit^{+} *Tnfsf13*$^{-/-}$ BM cells were transduced with a gamma retroviral vector expressing MLL-AF9 and transplanted into sublethally irradiated *Tnfsf13*$^{+/+}$ or *Tnfsf13*$^{-/-}$ recipient mice (Figure 5A). A 2.1-fold-lower (P<0.01) leukemic burden was detected in the PB of *Tnfsf13*$^{-/-}$ recipient mice six weeks post transplantation, but no significant survival difference was observed between the two groups (Figure 5B and C and *Online Supplementary Figure S5A and B*). To study whether TNFSF13 supports AML maintenance *in vivo*, 10,000 or 1,000 leukemia cells harvested from spleens of primary recipients of each group were transplanted into corresponding *Tnfsf13*$^{+/+}$ or *Tnfsf13*$^{-/-}$ secondary recipient mice (Figure 5A). Interestingly, while no significant difference in survival was observed between the groups when transplanting 10,000 leukemia cells (*Online Supplementary Figure S5C*), *Tnfsf13*$^{-/-}$ recipients showed an extended survival compared to *Tnfsf13*$^{+/+}$ recipients when 1,000 leukemia cells were transplanted (mean of 28.5 *vs.* 34.5 days; P=0.0235) (Figure 5D). These data indicate that TNFSF13 supports AML initiation and maintenance under physiological conditions.

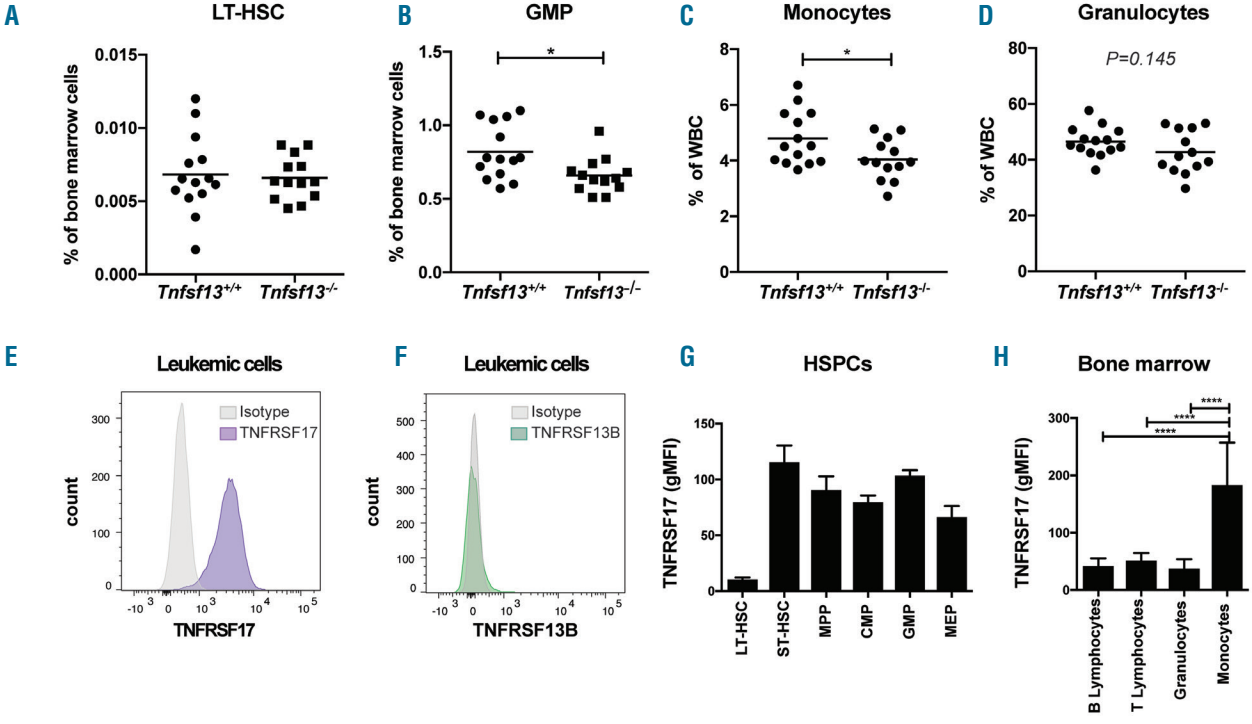

Figure 4. *Tnfsf13*$^{-/-}$ mice have myelopoiesis defects and acute myeloid leukemia cells express TNFRSF17. Frequency of (A) long-term hematopoietic stem cells (LT-HSC), (B) granulocyte and macrophage progenitor (GMP) cells, (C) monocytes, and (D) granulocytes in the bone marrow of *Tnfsf13*$^{+/+}$ (n=14) and *Tnfsf13*$^{-/-}$ (n=13) mice. Flow cytometric analysis showing (E) TNFRSF17 (purple) and (F) TNFRSF13B (green) expression on c-Kit^{+} MLL-AF9 leukemic cells. Isotype control is shown in light gray. TNFRSF17 geometric mean fluorescent intensity (gMFI) expression within (G) hematopoietic stem and progenitor cells (HSPC) (n=5) and (H) lineage populations (n=10) in the bone marrow of normal mice, after subtracting the signal using matching isotype control antibodies. Values are means±Standard Deviation. *P<0.05; ****P<0.0001. WBC: white blood cells.

To explore the biological mechanisms by which TNFSF13 promotes AML cells, we investigated whether TNFSF13 affects the apoptosis and cell cycle status of c-Kit$^+$ leukemia cells. We found that TNFSF13 stimulation had an anti-apoptotic effect, with both early and late apoptotic cells being reduced (Figure 6A and B). The anti-apoptotic effects were also accompanied by an increase in actively cycling cells (Figure 6C and D). Collectively, these data indicate that TNFSF13 supports AML cells by suppressing apoptosis and promoting active cell cycle progression.

TNFSF13 promotes human acute myeloid leukemia cells by suppressing apoptosis

To assess whether TNFSF13 also stimulates human AML cells, we analyzed the sensitivity of nine human myeloid leukemia cell lines to TNFSF13. Upon serum deprivation, we found that TNFSF13 significantly supported the growth and survival of six of the nine cell lines and TNFSF13 was confirmed to bind to the cell surface of the AML cells (Figure 7A and B and *Online Supplementary Figure S6A and B*). To efficiently bind to TNFRSF13B or TNFRSF17, TNFSF13 binds to heparan sulfate proteoglycans (HSPG), which facilitates TNFSF13 oligomerization.[18] In accordance with this, we detected expression of the proteoglycan SYNDECAN-1 (CD138) on Mono-Mac-6 cells (Figure 7C). Further, as previously described,[18,19] the binding of TNFSF13 to HSPG was blocked by heparin (Figure 7D). Moreover, consistent with the effect observed on murine c-Kit$^+$ leukemia cells, TNFSF13 stimulation suppressed apoptosis in the AML cell line Mono-Mac-6 (Figure 7E and *Online Supplementary Figure S6C*), but did not significantly affect the cell cycle (*Online Supplementary Figure S6D*). In accordance with murine AML cells, TNFRSF13B was not expressed on human AML cell lines, whereas TNFRSF17 was detected on 3 of 9 of the myeloid leukemia cell lines by flow cytometry, and in 7 of 9 of cell lines by real-time PCR, albeit at low levels (*Online Supplementary Figure S6E and H*).

To investigate which of the two receptors is the most prominent on AML patient cells, we analyzed their expression pattern in AML patient data from the TCGA database.[20] Similar to the c-Kit$^+$ murine leukemia cells and human cell line data, *TNFRSF17* was expressed at significantly higher levels than *TNFRSF13B* (*Online Supplementary Figure S6I*). In addition, we observed a higher relative expression of both *TNFRSF13B* and *TNFRSF17* in *RUNX1*-mutated (2.5- and 2.6-fold change, respectively) and *TP53*-mutated (3.5- and 3.2-fold change, respectively) AML patients, two genetic subtypes associated with a dismal outcome (*Online Supplementary Table S5*).[21-23] These findings demonstrate that TNFSF13 also promotes human AML cells *in vitro* by suppressing apoptosis, and suggest that TNFRSF17 is the primary receptor for TNFSF13 on human AML cells.

TNFSF13B promotes proliferation of human acute myeloid leukemia cells

We also evaluated the role of TNFSF13B (BAFF) in AML, another ligand for TNFRSF17. TNFSF13B levels were approximately 100-fold lower than TNFSF13 levels in the mouse BM (Figure 3B and *Online Supplementary Figure S7A*), whereas similar levels of the two cytokines were

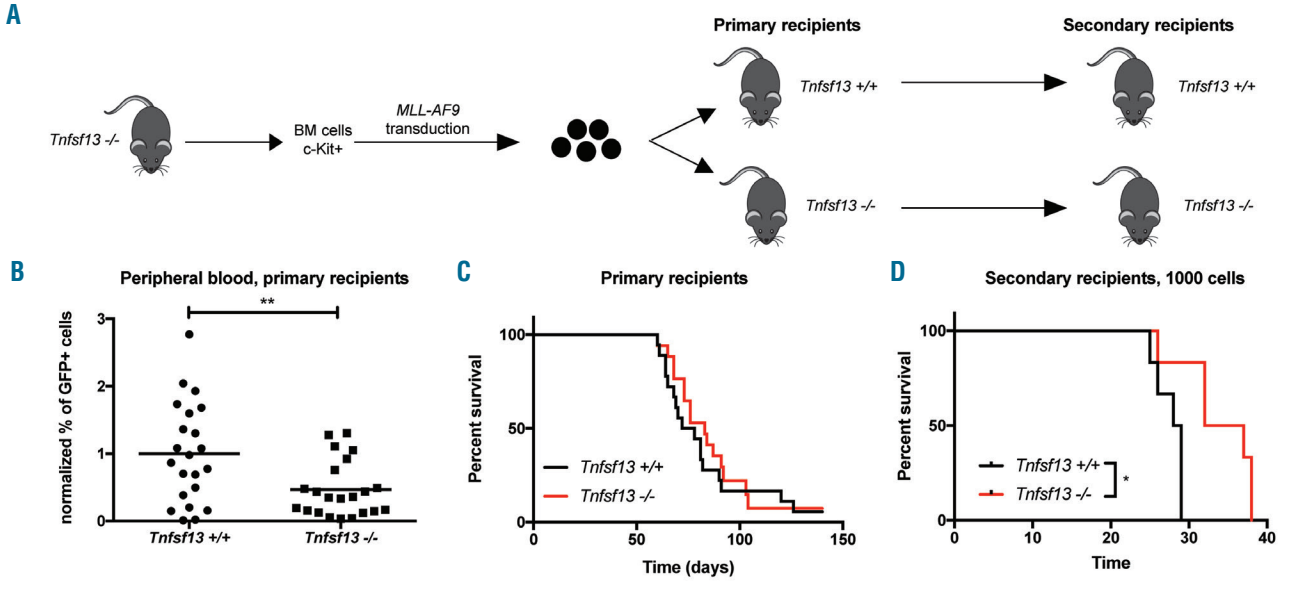

Figure 5. TNFSF13 supports leukemia development *in vivo*. A total of 250,000 c-Kit$^+$ bone marrow (BM) cells from *Tnfsf13*$^{-/-}$ mice were transduced with a MIG-*MLL-AF9* retroviral vector and transplanted into sublethally irradiated *Tnfsf13*$^{+/+}$ and *Tnfsf13*$^{-/-}$ primary recipient mice (22 mice per group, pooled from four independent experiments). 1,000 leukemia cells harvested from spleens of primary recipients were transplanted into secondary recipient mice with matching genetic background. (A) Schematic picture showing the experimental setup. (B) Percentage of leukemic (GFP$^+$) cells in the peripheral blood of the *Tnfsf13*$^{-/-}$ and *Tnfsf13*$^{+/+}$ recipient mice 40 days after transplantation, normalized to the mean of the control (*Tnfsf13*$^{+/+}$) group in each experiment. Horizontal lines show the mean values within groups. (C) Kaplan-Meier curves showing the survival of primary recipient mice. (D) Kaplan-Meier curves showing the survival of secondary recipient mice (6 mice per group; pooled data from 2 donors per group). *P<0.05; **P<0.01.

observed in plasma (Figure 3A and *Online Supplementary Figure S7B*). The c-Kit$^+$ murine leukemia cells did not show a significant response to TNFSF13B stimulation *in vitro* (*Online Supplementary Figure S7C*), but in human Mono-Mac-6 cells, TNFSF13B stimulation had similar effect as TNFSF13, resulting in increased cell number (*Online Supplementary Figure S7D*).

TNFSF13 supports acute myeloid leukemia cells in an NF-κB-dependent manner

To explore the molecular mechanism by which TNFSF13 promotes AML cell growth and survival, we generated RNA sequencing data of Mono-Mac-6 cells that had been stimulated with TNFSF13 for 24 hours. Consistent with TNFSF13 being a member of the tumor necrosis factor (TNF) superfamily, gene set enrichment analysis (GSEA) demonstrated an enriched TNF receptor activation signature upon TNFSF13 stimulation [false discovery rate (FDR) <0.10] (Figure 7F and *Online Supplementary Table S6*). Furthermore, an enriched NF-κB signature was evident in TNFSF13-stimulated cells (FDR<0.05) (Figure 7G and *Online Supplementary Table S6*) and phospho-flow cytometric analysis confirmed NF-κB activation upon TNFSF13 stimulation (Figure 7H). Consistent with this data, TNFSF13 stimulation resulted in a significant upregulation of the NF-κB target genes AGT, IRF1, IRF7, PTGDS, and VIM (*Online Supplementary Figure S8A*). By using a TNFRSF17 blocking antibody, TNFSF13-induced cell proliferation and NF-κB activation was hindered (Figure 7I and J), demonstrating that TNFSF13 activates NF-κB by binding to TNFRSF17. To assess whether TNFSF13 promotes cell proliferation by activating NF-κB, we inhibited NF-κB activation using TPCA1 and IKK-16, two selective inhibitors of IκB kinase (IKK).[24] Both TPCA1 and IKK-16 treatment inhibited NF-κB activation and reversed the effects of TNFSF13 in Mono-Mac-6 cells (Figure 7K and L and *Online Supplementary Figure S8B and C*). These data demonstrate that TNFSF13 supports the growth of human AML cells in an NF-κB-dependent manner.

Discussion

Although *in vivo* assays are critical to assess stem cell function, performing screens *in vivo* is challenging due to the large number of experimental animals needed to provide meaningful data. In this study, we developed arrayed molecular barcodes in lentiviral vectors, which enabled us to assess the effects of 114 cytokines on leukemia-initiat-

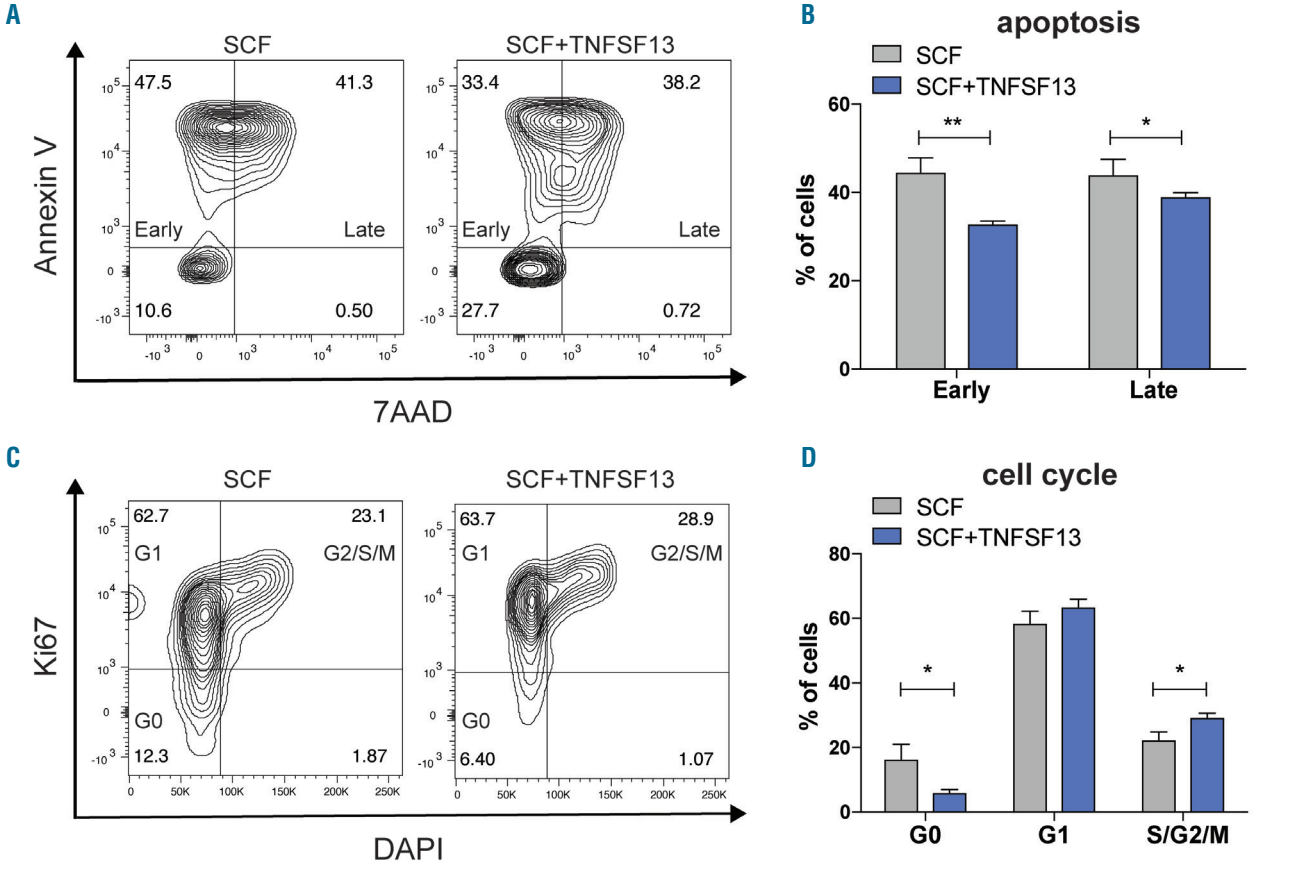

Figure 6. TNFSF13 maintains acute myeloid leukemia (AML) cells by suppressing apoptosis and promoting cell cycle progression. c-Kit$^+$ *MLL-AF9* AML cells were cultured for 3 days with stem cell factor (SCF) as a baseline and stimulated with TNFSF13 or no TNFSF13 (Control) prior to apoptosis and cell cycle analysis. (A) Representative contour plots showing Annexin-V and 7AAD staining. (B) Percentage of early (Annexin-V$^+$7AAD$^-$) and late (Annexin-V$^+$7AAD$^+$) apoptotic cells (n=3). (C) Representative contour plots showing Ki67 and DAPI staining. (D) Percentage of cells in G0, G1, or S/G2/M phase of the cell cycle (n=3) determined by Ki67 and DAPI staining. Values are means±Standard Deviation. *P<0.05; **P<0.01.

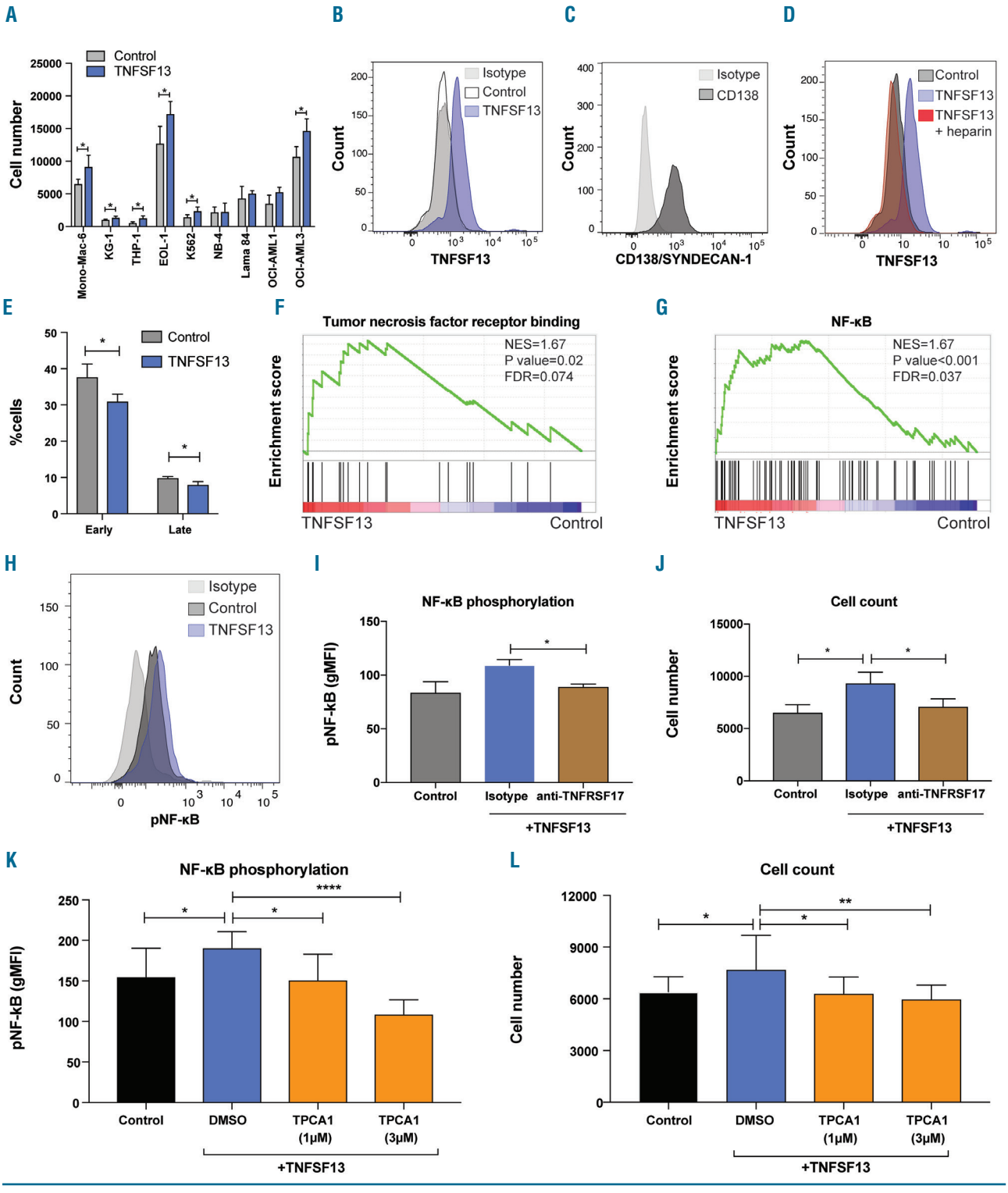

Figure 7. TNFSF13 promotes human acute myeloid leukemia cells in an NF-κB-dependent manner. (A) Output cell number of human myeloid leukemia cell lines cultured under serum-free conditions for three days with or without (Control) TNFSF13. A total of 1,000 cells were seeded per well (n=3). (B) Representative flow cytometric analysis showing staining of TNFSF13 on the cell surface of Mono-Mac-6 following 5-minute (min) stimulation with TNFSF13 (blue, 100 ng/mL) compared to non-stimulated cells (Control, white). Isotype control is shown in light gray. (C) Representative flow cytometric analysis showing SYNDECAN-1 (CD138) (dark gray) expression on Mono-Mac-6 cells. Isotype control is shown in light gray. (D) Representative flow cytometric analysis showing staining of TNFSF13 on the cell surface of Mono-Mac-6 following 5 min stimulation with TNFSF13 (100 ng/mL); with (red) or without (blue) heparin (4 IU/mL). Non-stimulated cells were used as control (white). (E) Percentage of early (Annexin-V$^+$7AAD$^-$) and late (Annexin-V$^+$7AAD$^+$) apoptotic Mono-Mac-6 cells following three days of stimulation with TNFSF13 (n=3). (F and G) Mono-Mac-6 cells were stimulated with TNFSF13 for 24 hours (h) prior to RNA sequencing. Gene Set Enrichment Analysis identified an enriched (F) TNF receptor signature (gene set from MsigDB, molecular signatures database) and an (G) NF-κB signature.[50] (H) Phospho-flow cytometric analysis of Mono-Mac-6 cells stimulated with TNFSF13 for 1 h. Isotype (light gray) and pNF-κB (Control, dark gray; TNFSF13, blue) staining. (I and J) Mono-Mac-6 cells were stimulated with TNFSF13 in the presence of a TNFRSF17 blocking antibody or corresponding isotype control, and analyzed for (I) pNF-κB expression after subtracting the signal using matching isotype control antibodies, and (J) output cell number after three days. (K and L) Mono-Mac-6 cells were treated with the IKK inhibitor TPCA1 at 1 or 3 μM during TNFSF13 stimulation and analyzed after three days for (K) pNF-κB expression after subtracting the signal using matching isotype control antibodies and (L) output cell number. Values are means±Standard Deviation. *P<0.05; **P<0.01; ****P<0.0001. FDR: false discovery rate; DMSO: dimethyl sulfoxide.

ing function using a competitive *in vivo* readout of leukemic cells. This approach significantly reduces the number of mice since leukemia cells from up to 11 different cytokine conditions can be pooled in each mouse. The arrayed barcoded approach is applicable to other types of *ex vivo* screens with *in vivo* readouts, as shown recently in a small-molecule screen using metastatic pancreatic cells.[25]

The barcoded cytokine screens identified IL9 and TNFSF13 as candidate positive regulators of leukemic-initiating cells. Validation experiments confirmed that both IL9 and TNFSF13 supported AML-initiating cells, but as TNFSF13 was more potent than IL9, we selected TNFSF13, a TNF superfamily ligand,[26] for further studies. The findings that *Tnfsf13*$^{-/-}$ recipient mice had lower leukemia burden and increased survival compared to controls following serial transplantations of leukemia cells suggest that TNFSF13 supports AML cells also under physiological condition. TNFSF13 has previously been shown to promote cancer-cell growth and survival of several types of solid tumors[27,28] and B-cell malignancies, such as acute lymphoblastic leukemia, Hodgkin lymphoma, and multiple myeloma.[26,29-32] In addition, elevated TNFSF13 levels have been found in multiple cancer types and are associated with a poor prognosis,[33] suggesting that TNFSF13 has broad tumor-promoting activity. Whereas the first *Tnfsf13*$^{-/-}$ mouse model generated did not reveal alterations in T- and B-cell development or *in vitro* function,[34] later studies of *Tnfsf13*$^{-/-}$ mice identified increased proliferation of T cells, changes in the secretion of immuno-cytokines, and impaired antibody class switching.[14,34]

In AML, TNFSF13 secretion has been linked to chemoresistance[36] and elevated TNFSF13 serum levels have been reported in patients,[36,37] but TNFSF13 has not previously been associated with AML stem cells or myelopoiesis. Given that the GMP cell stage is associated with AML initiation,[38] it was interesting to note that TNFRSF17 is expressed on myeloid progenitor cell populations and that *Tnfsf13*$^{-/-}$ mice have reduced numbers of GMP cells and monocytes, suggesting that TNFSF13 has a previously unrecognized role in myelopoiesis.

In agreement with previous studies showing that TNFSF13 is expressed by infiltrating neutrophils in solid tumors[39,40] and by myeloid BM cells in multiple myeloma,[41,42] we found that TNFSF13 was secreted by CD11b^{+}Gr-1^{+} myeloid cells but not by the corresponding murine AML cells. This finding suggests that mature myeloid BM cells support AML cells by secreting TNFSF13. In contrast to the findings in the murine MLL-AF9 AML model, TNFSF13 is expressed by leukemia cells in certain AML subtypes,[36,37] suggesting that TNFSF13 might play a more critical role for leukemia development and progression in these subtypes.

The anti-apoptotic effect induced by TNFSF13 is consistent with prior findings in B-cell malignancies[43-45] and glioma,[46] suggesting a similar mechanism induced by TNFSF13 in various types of cancers. Moreover, TNFSF13 promoted AML cells in an NF-κB-dependent manner, which is in agreement with studies showing that TNFSF13 activates NF-κB in multiple myeloma cells,[32] chronic lymphocytic leukemia,[30] and non-Hodgkin lymphoma B cells.[45] NF-κB signaling is elevated and critical for AML stem cells,[47,48] including MLL-rearranged AML cells, but the underlying mechanism causing NF-κB activation has not been clarified. Along with IL1-induced activation of NF-κB in primitive leukemia cells,[49] our findings suggest that TNFSF13 contributes to enhanced NF-κB activity in AML cells. Because AML cells from various AML subtypes lacking MLL rearrangements were also sensitive to TNFSF13, the effects of TNFSF13 stimulation are not restricted to MLL-rearranged AML.

In summary, we have established a cytokine screen using arrayed molecular barcoding of AML cells allowing for an *in vivo* competitive readout of leukemia-initiating activity. The screen provides a new strategy for studying the influence of secreted factors on AML-initiating cells. This approach identified TNFSF13 as a positive regulator of AML stem cells and showed that TNFSF13 promotes AML cells in an NF-κB-dependent manner. Moreover, we identified a role for TNFSF13 in normal myelopoiesis and showed that normal myeloid cells secrete TNFSF13. This study demonstrates the utility of using arrayed molecular barcoding as a new screening tool for identifying novel stem cell regulators.

Acknowledgments

This work was supported by the Swedish Cancer Society, the Swedish Childhood Cancer Foundation, the Crafoord Foundation, the Gunnar Nilsson Cancer Foundation, the Medical Faculty of Lund University, the Royal Physiographic Society of Lund, the Swedish Research Council, BioCARE, and FP7 Marie Curie.

References

1. Schepers K, Campbell TB, Passegué E. Normal and Leukemic Stem Cell Niches: Insights and Therapeutic Opportunities. Cell Stem Cell. 2015;16(3):254-267.
2. Morrison SJ, Scadden DT. The bone marrow niche for haematopoietic stem cells. Nature. 2014;505(7483):327-334.
3. Shlush LI, Mitchell A, Heisler L, et al. Tracing the origins of relapse in acute myeloid leukaemia to stem cells. Nature. 2017;547(7661):104-108.
4. Peña-Martinez P, Eriksson M, Ramakrishnan R, et al. Interleukin 4 induces apoptosis of acute myeloid leukemia cells in a Stat6-dependent manner. Leukemia. 2018;32(3):588-596.
5. Lu R, Neff NF, Quake SR, Weissman IL. Tracking single hematopoietic stem cells in vivo using high-throughput sequencing in conjunction with viral genetic barcoding. Nat Biotechnol. 2011;29(10):928-933.
6. Cheung AMS, Nguyen LV, Carles A, et al. Analysis of the clonal growth and differentiation dynamics of primitive barcoded human cord blood cells in NSG mice. Blood. 2013;122(18):3129-3137.
7. Grosselin J, Sii-Felice K, Payen E, Chretien S, Tronik-Le Roux D, Leboulch P. Arrayed lentiviral barcoding for quantification analysis of hematopoietic dynamics. Stem Cells. 2013;31(10):2162-2171.
8. Klauke K, Broekhuis MJC, Weersing E, et al. Tracing dynamics and clonal heterogeneity of Cbx7-induced leukemic stem cells by cellular barcoding. Stem Cell Rep. 2015;4(1):74-89.
9. Järås M, Miller PG, Chu LP, et al. Csnk1a1 inhibition has p53-dependent therapeutic efficacy in acute myeloid leukemia. J Exp Med. 2014;211(4):605-612.
10. Hartwell KA, Miller PG, Mukherjee S, et al. Niche-based screening identifies small-molecule inhibitors of leukemia stem cells. Nat Chem Biol. 2013;9(12):840-848.
11. Moffat J, Grueneberg DA, Yang X, et al. A lentiviral RNAi library for human and mouse genes applied to an arrayed viral high-content screen. Cell. 2006;124(6):1283-1298.
12. Xiao Y, Motomura S, Deyev V, Podack ER. TNF superfamily member 13, APRIL, inhibits allergic lung inflammation. Eur J Immunol. 2011;41(1):164-171.
13. Xiao Y, Motomura S, Podack ER. APRIL (TNFSF13) regulates collagen-induced

arthritis, IL-17 production and Th2 response. Eur J Immunol. 2008;38(12): 3450-3458.
14. Miller PG, Al-Shahrour F, Hartwell KA, et al. In Vivo RNAi Screening Identifies a Leukemia-Specific Dependence on Integrin Beta 3 Signaling. Cancer Cell. 2013; 24(1):45-58.
15. Puram RV, Kowalczyk MS, de Boer CG, et al. Core Circadian Clock Genes Regulate Leukemia Stem Cells in AML. Cell. 2016;165(2):303-316.
16. Wang Y-Y, Zhao L-J, Wu C-F, et al. C-KIT mutation cooperates with full-length AML1-ETO to induce acute myeloid leukemia in mice. Proc Natl Acad Sci U S A. 2011;108(6):2450-2455.
17. Bossen C, Schneider P. BAFF, APRIL and their receptors: Structure, function and signaling. Semin Immunol. 2006;18(5):263-275.
18. Ingold K, Zumsteg A, Tardivel A, et al. Identification of proteoglycans as the APRIL-specific binding partners. J Exp Med. 2005;201(9):1375-1383.
19. Hendriks J, Planelles L, de Jong-Odding J, et al. Heparan sulfate proteoglycan binding promotes APRIL-induced tumor cell proliferation. Cell Death Differ. 2005;12(6):637-648.
20. Ley TJ, Miller C, Ding L, et al. Genomic and epigenomic landscapes of adult de novo acute myeloid leukemia. N Engl J Med. 2013;368(22):2059-2074.
21. Papaemmanuil E, Gerstung M, Bullinger L, et al. Genomic Classification and Prognosis in Acute Myeloid Leukemia. N Engl J Med. 2016;374(23):2209–2221.
22. Gaidzik VI, Teleanu V, Papaemmanuil E, et al. RUNX1 mutations in acute myeloid leukemia are associated with distinct clinico-pathologic and genetic features. Leukemia. 2016;30(11):2160–2168.
23. Rucker FG, Schlenk RF, Bullinger L, et al. TP53 alterations in acute myeloid leukemia with complex karyotype correlate with specific copy number alterations, monosomal karyotype, and dismal outcome. Blood. 2012;119(9):2114-2121.
24. Podolin PL, Callahan JF, Bolognese BJ, et al. Attenuation of murine collagen-induced arthritis by a novel, potent, selective small molecule inhibitor of IkappaB Kinase 2, TPCA-1 (2-[(aminocarbonyl)amino]-5-(4-fluorophenyl)-3-thiophenecarboxamide), occurs via reduction of proinflammatory cytokines and antigen-induced T cell Proliferation. J Pharmacol Exp Ther. 2005;312(1):373-381.
25. Grüner BM, Schulze CJ, Yang D, et al. An in vivo multiplexed small-molecule screening platform. Nat Methods. 2016;13(10):883-889.
26. Hahne M, Kataoka T, Schroter M, et al. APRIL, a new ligand of the tumor necrosis factor family, stimulates tumor cell growth. J Exp Med. 1998;188(6):1185-1190.
27. García-Castro A, Zonca M, Florindo-Pinheiro D, et al. APRIL promotes breast tumor growth and metastasis and is associated with aggressive basal breast cancer. Carcinogenesis. 2015;36(5):574-584.
28. Wang R, Guo Y, Ma H, et al. Tumor necrosis factor superfamily member 13 is a novel biomarker for diagnosis and prognosis and promotes cancer cell proliferation in laryngeal squamous cell carcinoma. Tumour Biol. 2016;37(2):2635-2645.
29. Chiu A, Xu W, He B, et al. Hodgkin lymphoma cells express TACI and BCMA receptors and generate survival and proliferation signals in response to BAFF and APRIL. Blood. 2007;109(2):729-739.
30. Endo T, Nishio M, Enzler T, et al. BAFF and APRIL support chronic lymphocytic leukemia B-cell survival through activation of the canonical NF-kappaB pathway. Blood. 2007;109(2):703-710.
31. Quinn J, Glassford J, Percy L, et al. APRIL promotes cell-cycle progression in primary multiple myeloma cells: influence of D-type cyclin group and translocation status. Blood. 2011;117(3):890-901.
32. Tai Y-T, Acharya C, An G, et al. APRIL and BCMA promote human multiple myeloma growth and immunosuppression in the bone marrow microenvironment. Blood. 2016;127(25):3225-3236.
33. Moreaux J, Veyrune J-L, De Vos J, Klein B. APRIL is overexpressed in cancer: link with tumor progression. BMC Cancer. 2009; 9:83.
34. Varfolomeev E, Kischkel F, Martin F, et al. APRIL-deficient mice have normal immune system development. Mol Cell Biol. 2004;24(3):997-1006.
35. Castigli E, Scott S, Dedeoglu F, et al. Impaired IgA class switching in APRIL-deficient mice. Proc Natl Acad Sci U S A. 2004;101(11):3903-3908.
36. Bonci D, Musumeci M, Coppola V, et al. Blocking the APRIL circuit enhances acute myeloid leukemia cell chemosensitivity. Haematologica. 2008;93(12):1899-1902.
37. Bolkun L, Lemancewicz D, Jablonska E, et al. The impact of TNF superfamily molecules on overall survival in acute myeloid leukaemia: correlation with biological and clinical features. Ann Hematol. 2015; 94(1):35-43.
38. Krivtsov AV, Twomey D, Feng Z, et al. Transformation from committed progenitor to leukaemia stem cell initiated by MLL–AF9. Nature. 2006;442(7104):818-822.
39. Jablonska E, Wawrusiewicz-Kurylonek N, Garley M, et al. A proliferation-inducing ligand (APRIL) in neutrophils of patients with oral cavity squamous cell carcinoma. Eur Cytokine Netw. 2012;23(3):93-100.
40. Schwaller J, Schneider P, Mhawech-Fauceglia P, et al. Neutrophil-derived APRIL concentrated in tumor lesions by proteoglycans correlates with human B-cell lymphoma aggressiveness. Blood. 2007; 109(1):331-338.
41. Matthes T, Dunand-Sauthier I, Santiago-Raber M-L, et al. Production of the plasma-cell survival factor a proliferation-inducing ligand (APRIL) peaks in myeloid precursor cells from human bone marrow. Blood. 2011;118(7):1838-1844.
42. Matthes T, McKee T, Dunand-Sauthier I, et al. Myelopoiesis dysregulation associated to sustained APRIL production in multiple myeloma-infiltrated bone marrow. Leukemia. 2015;29(9):1901-1908.
43. Kern C, Cornuel J-F, Billard C, et al. Involvement of BAFF and APRIL in the resistance to apoptosis of B-CLL through an autocrine pathway. Blood. 2004;103 (2):679-688.
44. Moreaux J, Legouffe E, Jourdan E, et al. BAFF and APRIL protect myeloma cells from apoptosis induced by interleukin 6 deprivation and dexamethasone. Blood. 2004;103(8):3148-3157.
45. He B, Chadburn A, Jou E, Schattner EJ, Knowles DM, Cerutti A. Lymphoma B cells evade apoptosis through the TNF family members BAFF/BLyS and APRIL. J Immunol. 2004;172(5):3268-3279.
46. Roth W, Wagenknecht B, Klumpp A, et al. APRIL, a new member of the tumor necrosis factor family, modulates death ligand-induced apoptosis. Cell Death Differ. 2001;8(4):403-410.
47. Kuo H-P, Wang Z, Lee D-F, et al. Epigenetic roles of MLL oncoproteins are dependent on NF-kappaB. Cancer Cell. 2013;24(4): 423-437.
48. Bosman MCJ, Schepers H, Jaques J, et al. The TAK1-NF-kappaB axis as therapeutic target for AML. Blood. 2014;124(20):3130-3140.
49. Ågerstam H, Hansen N, von Palffy S, et al. IL1RAP antibodies block IL-1-induced expansion of candidate CML stem cells and mediate cell killing in xenograft models. Blood. 2016;128(23):2683-2693.
50. Pahl HL. Activators and target genes of Rel/NF-kappaB transcription factors. Oncogene. 1999;18(49):6853-6866.